Evolution of spherical overdensities in energy-momentum-squared gravity

Bita Farsi,[1,*] Ahmad Sheykhi,[1,2,†] and Mohsen Khodadi[1,2,‡]
[1]*Department of Physics, College of Sciences, Shiraz University, Shiraz 71454, Iran*
[2]*Biruni Observatory, College of Sciences, Shiraz University, Shiraz 71454, Iran*

(Received 7 April 2023; accepted 11 July 2023; published 25 July 2023)

Employing the spherical collapse formalism, we investigate the linear evolution of the matter overdensity for energy-momentum-squared gravity (EMSG), which in practical phenomenological terms one may imagine as an extension of the ΛCDM model of cosmology. The underlying model, while still having a cosmological constant, is a nonlinear material extension of the general theory of relativity and includes correction terms that are dominant in the high-energy regime, the early Universe. Considering the Friedmann-Robertson-Walker background in the presence of a cosmological constant, we find the effects of the modifications arising from EMSG on the growth of perturbations at the early stages of the Universe. Considering both possible negative and positive values of the model parameter of EMSG, we discuss its role in the evolution of the matter density contrast and growth function in the level of linear perturbations. While EMSG leaves imprints distinguishable from ΛCDM, we find that the negative range of the EMSG model parameter is not well behaved, indicating an anomaly in the parameter space of the model. In this regard, for the evaluation of the galaxy cluster number count in the framework of EMSG, we equivalently provide an analysis of the number count of the gravitationally collapsed objects (or the dark matter halos). We show that the galaxy cluster number count decreases compared to the ΛCDM model. In agreement with the hierarchical model of structure formation, in EMSG cosmology the more massive structures are less abundant, meaning that they form at later times.

DOI: 10.1103/PhysRevD.108.023524

I. INTRODUCTION

It is not an exaggeration to say that the discovery of the current cosmic acceleration of the Universe is the most exciting cosmological achievement in many decades. Generally speaking, it implies that the Universe is dominated by an enigmatic repulsive force, so-called dark energy (DE) with unusual physical properties, or that the general theory of relativity (GTR) as the basis of standard cosmology (ΛCDM) fails on cosmological scales [1]. This enigmatic force has inspired many researchers to reveal its unknown properties. In this regard, serving alternative theories of gravity that indeed are extensions of GTR are regarded as the most optimistic proposals to disclose the nature of the accelerating expansion of the Universe. In addition to DE, there are other unresolved issues, such as the explanation of the missing matter is known as dark matter (DM) at the galactic and cosmological scales, and the existence of singularities at high-energy regimes which keep open the way to going beyond GTR (see Ref. [2] for more knowing). In the review paper [3], one can find a systematic discussion on some standard issues and the latest developments of modified gravity in cosmology.

Usually, the theories beyond GTR build due by adding scalar invariants (also their corresponding functions) in the geometric section of the Einstein-Hilbert action. The most simple modification of GTR is the so-called $f(R)$ theory, in which the Ricci scalar R takes different forms. The viable aspects of these alternative theories have been comprehensively discussed in the literature [4]. In the continuation of this road, a generalization of $f(R)$ theory of gravity has been suggested in Ref. [5] known as $f(R,T)$ gravity, where T denotes the trace of the energy-momentum tensor (EMT). The outstanding feature of $f(R,T)$ theories, which are also known as minimal curvature-matter coupling models,[1] is that they can provide worthy descriptions for the late-time cosmic acceleration and the interconnection of DE, and DM, as well (see e.g., [7–9]). Note that some of the classes of $f(R,T)$ gravity also suffer from inviability issues and cannot provide a realistic cosmology [10]. Authors in [11], for the first time, developed theories exploiting the trace of EMT in the general form $f(R,(T_{\mu\nu}T^{\mu\nu})^n)$ $(0<n\leq 1)$, as the models violating the local or covariant energy-momentum conservation with the norm of EMT $T_{\mu\nu}T^{\mu\nu}$. Generally,

*Bita.Farsi@shirazu.ac.ir
†asheykhi@shirazu.ac.ir
‡m.khodadi@hafez.shirazu.ac.ir

[1]There is also the nonminimal version of the interaction between geometry and matter which is labeled as $f(R,T,R_{\mu\nu}T^{\mu\nu})$ [6].

these models are categorized under the name of energy-momentum-powered gravity, so that Ref. [11] by focusing only on two cases $n = 1/4$ and $1/2$ showed that the addition of the norm of EMT to the action results in the Cardassian expansion.[2] Further studies explicitly revealed to us that case $n < 1/2$ will affect the dynamic of the Universe in late time [13] while $n > 1/2$ is efficient to high-energy regimes [14,15]. Case $n = 1/2$ is very interesting in the sense that it affects the field equations independent of the energy density scale (see the cosmological and gravitational implications of this case in [16–18]).

With these prerequisites, since the topic under investigation in this paper, i.e., structure formation, is influenced by the dynamic governing the early Universe, then we take the case $n = 1$, which the authors in Refs. [14,15] have presented as a new covariant generalization of GTR relevant to the high-energy phase of the Universe. The label of this model is energy-momentum-squared gravity (EMSG) so that inducing the quadratic contributions to gravity from the matter side makes the appearance of new forms of fluid stresses, such as the scalar field and so on, unnecessary [19]. In general, $f(R, (T_{\mu\nu}T^{\mu\nu})^n)$ gravities enjoy this feature that their modifications do not come from gravitational Lagrangian but from the matter Lagrangian, unlike $f(R)$ theories. In other words, the self-coupling of the matter this time instead of geometry is supposed to give us interesting cosmological outputs, in particular, concerning the early Universe (case $n = 1$). Studies conducted in Refs. [14,20] (see also relevant papers [21,22]), respectively, indicate that EMSG in the context of bounce[3] and emergent scenarios is an alternative gravity without initial singularity. It may be justified by the fact that EMSG, similar to most quantum gravity approaches, predicts a minimum length and a finite maximum energy density, leading to a circumvention of the initial singularity problem in GTR. Due to some modifications induced by EMSG for the physics of the early Universe, one can consider it a phenomenological effort to improve the usual paradigm in ΛCDM-based cosmology. This idea, for several reasons, is justifiable. First, ΛCDM, due to the theoretical inconsistencies related to the cosmological constant, cannot provide us with a self-consistent description of cosmic acceleration, although it is successful in fitting a range of the observational data [25,26]. Second, some data analyses indicate incompatibilities between the ΛCDM prediction and the constraints obtained from some local observations; e.g., see Refs. [27–29]. Third, the Hubble tension that has recently been at the center of attention of the cosmology community warns us of the possibility of the invalidity of the ΛCDM picture of the early Universe [30–32]. It would be helpful to note that, despite the possibility of solving the cosmological constant issue at the late time via presenting quintessence DE, some studies show that it may make Hubble tension worse [33,34]. With this background, one may potentially take the EMSG as phenomenological extensions of the ΛCDM for the description of the early Universe, such that the additional free parameter appearing in Einstein's equations (arising from the nonlinear matter Lagrangian) finally can be constrained via cosmological observations. About the late-time behavior of EMSG cosmology, a recent study [35], by taking into consideration the homogenous and isotropic spacetime in the presence of the cosmological constant for this theory, succeeded in deriving different plausible scenarios of dark energy. Notably, one of these scenarios via presenting quintessence DE was able to solve the cosmological constant issue at the late time. In light of some cosmological observation measurements [36,37] and gravitational setups [19,38,39] derived different constraints for the free parameter of EMSG. Apart from these cases, we see EMSG in recent years subjected to evaluation in different contexts; see Refs. [40–48].

The structure formation of the Universe is highly sensitive to the accelerated expansion history of the Universe since any change affects the rate of formation and growth of collapsed structures [49]. This is important because all galaxies, quasars, and supernovae, in essence, come from collapsed structures, and their distribution in size, space, and time is subsequently affected. Indeed, large-scale structures in our current Universe are nothing but growing small fluctuations in the early Universe. This statement is valid for any source of changes in the expansion history of the Universe. With this idea in mind, we are going to study linear structure formation in cosmologies beyond standard ΛCDM, in particular, EMSG cosmology. The higher-order matter source terms appearing in the EMSG dynamical equations are expected to leave significant effects on the initial small fluctuations as well as the evolution of the structure. An appropriate approach to describe this evolution is known as top-hat spherical collapse (SC) formalism which addresses the growth of perturbations and subsequently structure formation [50]. In this approach, one considers a homogeneous and spherical symmetric perturbation in an expanding background and describes the growth of perturbations in a spherical region using the same Friedmann equations for the underlying theory of gravity [51–56]. More precisely, the top hat describes a homogeneous overdensity sphere that is, in principle, modeled by a discrete Friedmann-Robertson-Walker (FRW) closed universe lying in an external FRW universe, with flat spatial curvature [57]. The radius of this overdensity sphere

[2] It is a kind of expansion for the flat universe consisting of only matter and radiation (without vacuum contribution) and still consistent with observations [12].

[3] There is another analysis also that shows EMSG cannot replace the standard initial singularity with a regular bounce, meaning that it still suffers from geodesically incompleteness issue [23]. However, this problem can be solved in case of the existence of a vacuum energy density in EMSG [24].

expands at a rate slower than the background, gradually slowing down so that it finally reaches its possible maximum size, and then reversely shrinks into itself to collapse. Notably, our work here differs from [58], which has utilized the Newtonian gauge, since we instead serve SC formalism to survey the evolution of perturbations. It is worth noting that recently in the framework of EMSG, by investigating the dynamics of SC for a spherically symmetric configuration such as a star, the stability of self-gravitating objects has been addressed [59].

The outline of this paper is as follows. In Sec. II, we provide a review on EMSG and derive the corresponding Friedmann equations. In Sec. III, using the spherically collapse approach, we explore the growth of matter perturbation in the background of flat EMSG-based cosmology. In Sec. IV, for the existing cosmology framework we address the mass function and number count of the collapsed objects. We also devote the conclusion and discussion to the last Sec. V. In what follows we work in the units $\hbar = c = \kappa = 1$.

II. MODIFIED DYNAMIC EQUATIONS OF EMSG

In Ref. [15], the modified action of the EMSG model in the presence of the cosmological constant Λ is presented in the following form:

$$S_{EMSG} = \frac{1}{2\kappa}\int \sqrt{-g}\{F(R,T^2) - 2\Lambda + L_m\}d^4x, \quad (1)$$

with $F(R,T^2) = R + \eta T^2$, where $\kappa = 8\pi G/c^4$, and $T^2 \equiv T_{\mu\nu}T^{\mu\nu}$ is the scalar formed from the square of EMT. The action of matter also labels with L_m. Here, η is the model parameter denoting the coupling between matter and geometry with SI unite s^4kg^{-2}. Without going into detail, the Einstein's equation reads as

$$\begin{aligned} G_{\mu\nu} + \Lambda g_{\mu\nu} &= \kappa((\rho+p)u_\mu u_\nu + p g_{\mu\nu}) \\ &\quad + \eta\left(\frac{1}{2}(\rho^2+3p^2)g_{\mu\nu} + (\rho+p)(\rho+3p)u_\mu u_\nu\right). \quad (2) \end{aligned}$$

The first term in the right-hand side of the equation above shows the matter content described by a perfect fluid with the standard EMT $T_{\mu\nu}$, containing the energy density ρ and the pressure p which are connected via equation-of-state parameter $\omega = p/\rho$. As is clear from the second term, EMSG induces the quadratic contributions to gravity from matter terms which causes the standard EMT to be no longer conserved locally, i.e., $\nabla_\mu T^{\mu\nu} \neq 0$ (in [20] one can find more discussion on handling this issue). Note that here for perfect fluid we utilized the standard Lagrangian density $L_m = p$.

The modified Friedmann equations for the spatially homogeneous and flat FRW metric

$$ds^2 = -dt^2 + a^2(t)[dr^2 + r^2(d\theta^2 + \sin^2\theta d\phi^2)] \quad (3)$$

take the following forms [15]:

$$\left(\frac{\dot{a}}{a}\right)^2 = \frac{\Lambda}{3} + \frac{\rho}{3} + \frac{\eta\rho^2}{6}(3\omega^2 + 8\omega + 1), \quad (4)$$

$$\frac{\ddot{a}}{a} = \frac{\Lambda}{3} - \frac{1+3\omega}{6}\rho - \frac{\eta\rho^2}{3}(3\omega^2 + 2\omega + 1). \quad (5)$$

An interesting point in the above modified Friedmann equations is that in case of choosing $\eta < 0$ ($\eta > 0$), one can recover the effective Friedmann equations released in loop quantum cosmology [60] (braneworld cosmologies [61]). In this regard, by differentiating the Friedmann equations, the relevant continuity equation is acquired as

$$\dot{\rho} = -3\frac{\dot{a}}{a}\rho(1+\omega)\frac{1+\eta\rho(1+3\omega)}{1+\eta\rho(3\omega^2+8\omega+1)}, \quad (6)$$

which ρ indeed is the energy density of both baryonic and DM.

By taking the case of dust matter in the form of $p = p_m = 0$, $\omega_m = 0$, and $\rho = \rho_m$, Eqs. (4) and (5) can be reexpressed as

$$3H^2 = \Lambda + \rho_m + \frac{\eta}{2}\rho_m^2, \quad (7)$$

$$2\dot{H} + 3H^2 = \Lambda - \frac{\eta}{2}\rho_m^2. \quad (8)$$

We note that in the GTR limit (i.e., $\eta = 0$), the standard Friedmann equations will be recovered from Eqs. (7) and (8). The continuity equation (6) also for the underlying case leads to the usual behavior for the matter density as

$$\dot{\rho_m} + 3H\rho_m = 0. \quad (9)$$

The energy density of the pressureless matter ($p_m = 0$) can be obtained as $\rho_m = \rho_{m,0}a^{-3}$. The density parameters are given by

$$\Omega_\Lambda = \frac{\Lambda}{3H^2}, \quad (10)$$

$$\Omega_m = \frac{\rho_m}{3H^2}, \quad (11)$$

$$\Omega_\eta = \frac{\eta\rho_m^2}{6H^2}. \quad (12)$$

By substituting Eqs. (10)–(12) in Eq. (7) we obtain the following expression for the normalized Hubble parameter:

$$E(z) = \frac{H(z)}{H_0} = \sqrt{\Omega_{\Lambda,0} + \Omega_{m,0}(1+z)^3 + \Omega_{\eta,0}(1+z)^6}. \quad (13)$$

By taking this fact into account that at the present-time Universe $E(z=0)=1$, from Eq. (13), one gets the following relation between density parameters:

$$\Omega_{m,0} + \Omega_{\Lambda,0} = 1 - \Omega_{\eta,0}. \quad (14)$$

By relaxing η, the standard density equation is recovered, as expected. In light of the strong evidence that the Universe is Euclidean, and the total density parameter is $\Omega \equiv \Omega_m + \Omega_\Lambda = 1$, thereby, the value of the EMSG model parameter η should be tiny.

In Fig. 1 is plotted $E(z) - z$ for different values of η. As we can see, in EMSG cosmology, the normalized Hubble parameter decreases by moving from negative values of the model parameter η to positive ones. Also, for $\eta > 0$ ($\eta < 0$), the normalized Hubble parameter has a lower (steeper) slope, meaning that the rate of expansion of the Universe becomes slower (faster) relative to the standard ΛCDM model.

From Eqs. (7), (9), and (11), the evolution of the density abundance Ω_m can be written:

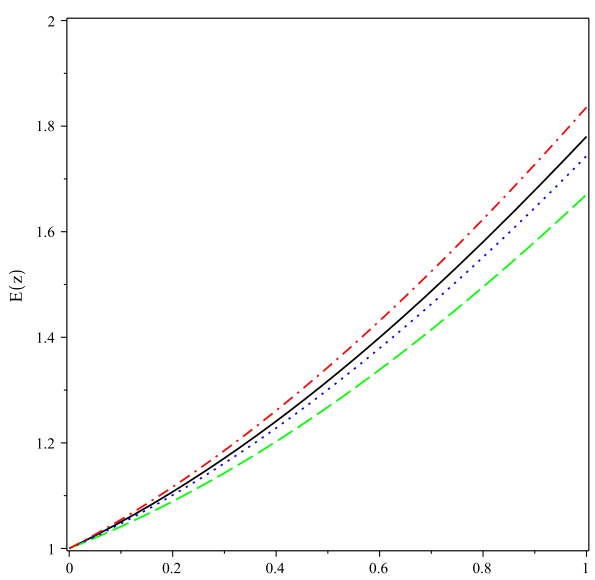

FIG. 1. The behavior of the normalized Hubble rate $E(z)$ as a function of redshift z for different values of EMSG model parameter η: $\eta = 0$ (ΛCDM, black solid line), $\eta = 10^{-5}$ (blue dotted line), $\eta = 10^{-4}$ (green dashed line), and $\eta = -10^{-5}$ (red dash-dotted line).

$$\Omega_m(z) \equiv \frac{\rho_m}{3H^2} = \frac{\rho_{m,0}(1+z)^3}{\rho_{m,0}(1+z)^3[1+\frac{\eta}{2}\rho_{m,0}(1+z)^3]+\Lambda} = \frac{\Omega_{m,0}}{\Omega_{m,0}+(1-\Omega_{m,0}-\Omega_{\Lambda,0})(1+z)^3+\Omega_{\Lambda,0}(1+z)^{-3}}. \quad (15)$$

In a similar manner, from Eqs. (7), (9), and (10), the evolution of the density abundance Ω_Λ takes the following form:

$$\Omega_\Lambda(z) \equiv \frac{\Lambda}{3H^2} = \frac{\Lambda}{\rho_{m,0}(1+z)^3[1+\frac{\eta}{2}\rho_{m,0}(1+z)^3]+\Lambda} = \frac{\Omega_{\Lambda,0}(1+z)^{-3}}{\Omega_{m,0}+(1-\Omega_{m,0}-\Omega_{\Lambda,0})(1+z)^3+\Omega_{\Lambda,0}(1+z)^{-3}}. \quad (16)$$

Also, using Eqs. (7), (9), and (12), for the evolution of the density abundance Ω_η we have

$$\Omega_\eta(z) \equiv \frac{\eta\rho_m^2}{6H^2} = \frac{\eta}{2}\frac{\rho_{m,0}^2(1+z)^6}{\rho_{m,0}(1+z)^3[1+\frac{\eta}{2}\rho_{m,0}(1+z)^3]+\Lambda} = \frac{\Omega_{\eta,0}(1+z)^6}{\Omega_{m,0}(1+z)^3+\Omega_{\eta,0}(1+z)^6+\Omega_{\Lambda,0}} = \frac{(1-\Omega_{m,0}-\Omega_{\Lambda,0})(1+z)^3}{\Omega_{m,0}+(1-\Omega_{m,0}-\Omega_{\Lambda,0})(1+z)^3+\Omega_{\Lambda,0}(1+z)^{-3}}. \quad (17)$$

The deceleration parameter in terms of the redshift can be written as

$$q = -1 - \frac{\dot{H}}{H^2} = -1 + \frac{(1+z)}{H(z)}\frac{dH(z)}{dz} = \frac{-2\Omega_{\Lambda,0}+\Omega_{m,0}(1+z)^3+4(1-\Omega_{\Lambda,0}-\Omega_{m,0})(1+z)^6}{2\Omega_{\Lambda,0}+2\Omega_{m,0}(1+z)^3+2(1-\Omega_{\Lambda,0}-\Omega_{m,0})(1+z)^6}. \quad (18)$$

One can see immediately that if $\eta = 0, \Lambda = 0$, then Eq. (18) reproduces exactly the GTR value, i.e., $q = 1/2$. We depict the behavior of the deceleration parameter q for different η in Fig. 2. It reveals to us that the Universe experiences a transition from decelerating phase ($z > z_{tr}$) to the accelerating phase ($z < z_{tr}$), where z_{tr} is the redshift at which the deceleration parameter vanishes. We see that with decreasing η (from positive to negative values), the phase transition between deceleration and acceleration takes place at lower redshifts. To clearly illustrate the role of the EMSG model parameter η, the values of z_{tr} are larger (smaller) than the ΛCDM model for $\eta > 0 (\eta < 0)$, meaning that for $\eta < 0$, this transition occurs later. Overall, from the combination of the results of Figs. 1 and 2, it can be said that

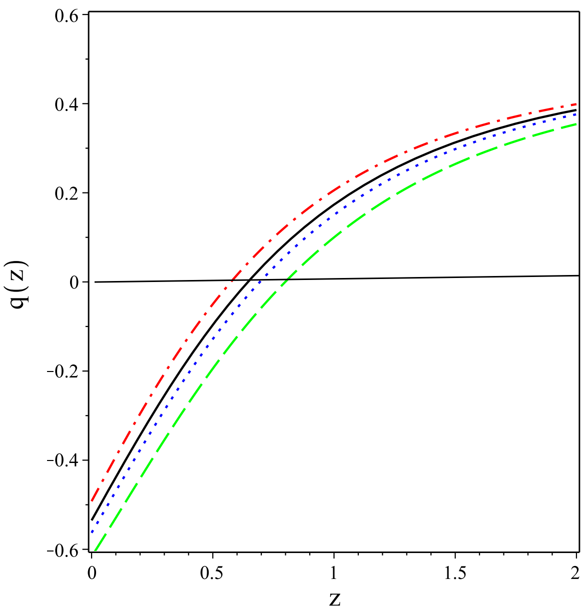

FIG. 2. The behavior of the deceleration parameter $q(z)$ as a function of redshift z for different values of the EMSG model parameter η: $\eta = 0$ (ΛCDM, black solid line), $\eta = 10^{-5}$ (blue dotted line), $\eta = 10^{-4}$ (green dashed line), and $\eta = -10^{-5}$ (red dash-dotted line).

$\eta > 0$ ($\eta < 0$) causes the Universe to experience an accelerated phase sooner (later) but with the expansion rate slower (faster) compared to the ΛCDM model.

III. SPHERICAL COLLAPSE IN EMSG-SETUP

By considering a dust fluid as the only constituent of the Universe (i.e., $p = p_m = 0$), Eq. (9) leads to

$$\dot{\rho}_m + 3H\rho_m = 0, \tag{19}$$

with a solution in the form $\rho_m = \rho_{m,0}a^{-3}$ in which $\rho_{m,0}$ denotes the energy density at the present time. To investigate the growth of perturbations, we take a spherically symmetric perturbed cloud of radius a_p, with a homogeneous energy density ρ_m^c. The SC model due to describing a spherical region with a top-hat profile and uniform density lets us write $\rho_m^c(t) = \rho_m(t) + \delta\rho_m$, at any time t [53]. Here we are faced with two cases $\delta\rho_m > 0$ and $\delta\rho_m < 0$. While for the former, this spherical region will eventually collapse under its gravitational force, for the latter, it will expand faster than the average Hubble expansion rate, subsequently generating a void. In other words, these two cases happen in overdense and underdense regions, respectively. Namely, in the matter-dominated Universe, denser regions expand slower than the rest of the Universe, which means if their density is large enough, they finally collapse and make clusters and other gravitational-bound systems [62]. Like Eq. (19), the continuity equation for the spherical region also takes the following form:

$$\dot{\rho}_m^c + 3h\rho_m^c = 0, \qquad h = \dot{a}_p/a_p, \tag{20}$$

where h refers to the local expansion rate of the spherical region with perturbed radius a_p. In line with our goal, let us start with the definition of density contrast as [62]

$$\delta_m = \frac{\rho_m^c}{\rho_m} - 1 = \frac{\delta\rho_m}{\rho_m}, \tag{21}$$

where ρ_m^c and ρ_m are the energy density of spherical perturbed cloud and the background density, respectively. Note that the advantage of the above definition is that it allows us to work with dimensionless quantities. It, in essence, measures the deviation of the local fluid density from the background density. Now, by taking the first and second time derivatives of Eq. (21), we respectively have

$$\dot{\delta}_m = 3(1 + \delta_m)(H - h), \tag{22}$$

$$\ddot{\delta}_m = 3(\dot{H} - \dot{h})(1 + \delta_m) + \frac{\dot{\delta}_m^2}{1 + \delta_m}, \tag{23}$$

where the dot denotes the derivative with respect to time. To estimate the second term of the above equation, $(\dot{H} - \dot{h})$, we use Eqs. (7) and (8) for the background and local regions, i.e.,

$$\frac{\ddot{a}}{a} = \frac{\Lambda}{3} - \frac{\rho_m}{6} - \frac{\eta}{3}\rho_m^2. \tag{24}$$

$$\frac{\ddot{a}_p}{a_p} = \frac{\Lambda}{3} - \frac{\rho_m^c}{6} - \frac{\eta}{3}(\rho_m^c)^2. \tag{25}$$

Despite that one may expect η to differ inside and outside of the spherical region, for simplicity here we suppose that $\eta^c = \eta$. From Eqs. (21), (24), and (25), one comes to

$$\dot{H} - \dot{h} = \frac{1}{6}\rho_m\delta_m + \frac{2}{3}\eta\rho_m^2\delta_m - H^2 + h^2. \tag{26}$$

Now, by combining Eqs. (26) in (23), and using (22), one gets the following differential equation for the density contrast modified by EMSG model parameter η:

$$\ddot{\delta}_m + 2H\dot{\delta}_m - \frac{1}{2}\rho_m\delta_m - 2\eta\rho_m^2\delta_m = 0. \tag{27}$$

The differential equation above is written in terms of a time derivative, and as usual, we should rewrite it in the form of the derivative in terms of the scale factor a. To do so, we introduce the following equations in which the prime represents the derivative in terms of the scale factor a:

$$\dot{\delta}_m = \delta_m' aH, \qquad \ddot{\delta}_m = \delta_m'' a^2H^2 + aH^2\delta_m' + a\dot{H}\delta_m'. \tag{28}$$

Using Eqs. (7) and (24),

$$\dot{H} = -\frac{1}{2}\rho_m - \frac{1}{2}\eta\rho_m^2, \tag{29}$$

and substituting it in Eq. (28), we arrive at

$$\ddot{\delta}_m = \delta_m'' a^2 H^2 + aH^2\delta_m' - \frac{a}{2}\rho_m(1+\eta\rho_m)\delta_m'. \tag{30}$$

Now by combining Eq. (27) with Eqs. (28) and (30), after ignoring the terms containing $O(\delta_m^2)$, and $O(\delta_m'^2)$, we have

$$\delta_m'' + \frac{3}{a}\delta_m' - \frac{1}{2aH^2}\rho_m(1+\eta\rho_m)\delta_m' - \frac{1}{2a^2H^2}\rho_m(1+4\eta\rho_m)\delta_m = 0. \tag{31}$$

Finally by putting H^2 from Eq. (7) in Eq. (31), we deal with the following differential equation:

$$\delta_m'' + \frac{3}{a}\delta_m' - \frac{3}{2a}\times\frac{\rho_m+\eta\rho_m^2}{\Lambda+\rho_m+\frac{\eta}{2}\rho_m^2}\delta_m' - \frac{3}{2a^2}\times\frac{\rho_m+4\eta\rho_m^2}{\Lambda+\rho_m+\frac{\eta}{2}\rho_m^2}\delta_m = 0. \tag{32}$$

One openly can see that in the absence of the EMSG model parameter ($\eta = 0$) and cosmological constant ($\Lambda = 0$), the perturbed equation for the density contrast, δ_m, in the linear regime, coincides with the ones in the GTR cosmology [49]:

$$\delta_m'' + \frac{3}{2a}\delta_m' - \frac{3\delta_m}{2a^2} = 0. \tag{33}$$

In Fig. 3, within the range $10 < z < 20$ of redshift, we have plotted the matter density contrasts as a function of z for the different values of the EMSG model parameter η. We observe that the EMSG cosmology leaves distinguishable imprints from ΛCDM on the density contrast of matter. More exactly, in the presence of η, the density contrast of matter starts growing from its initial value so that, in an expanding Universe, its growth is faster than the ΛCDM profile. However, Fig. 3 reflects an inconsistency in the behavior of $\eta < 0$. Although we see for $\eta > 0$ as it decreases, the growth of matter disturbances becomes slower and eventually goes to the ΛCDM model, for $\eta < 0$, the opposite happens, and the matter perturbations grow faster. In light of Fig. 3, we expect that with the increase of the η parameter, the matter perturbations will grow faster so that the behavior of $\eta < 0$ is nothing but an anomaly.[4] Then, from now on, we ignore it in our considerations and limit ourselves to the positive range of η. In general, quadratic contribution added to gravity from the

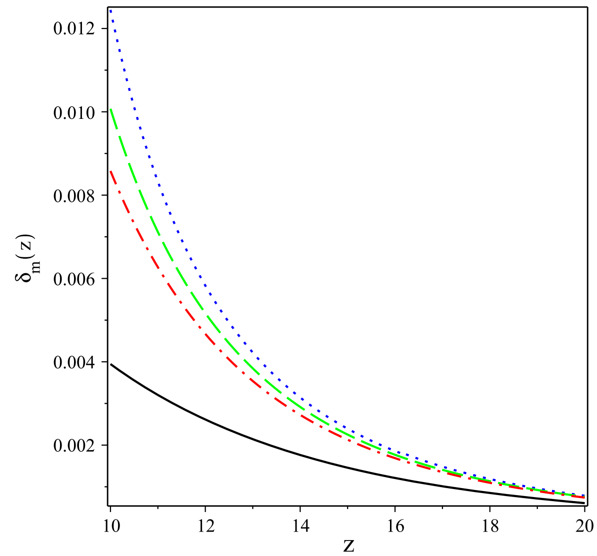

FIG. 3. The evolution of the matter density contrast for different values of η during the evolution of the Universe. We have chosen $\delta_m(z_i) = 0.0001$, $z_i = 400$, with different values for the EMSG model parameter η: $\eta = 0$ (ΛCDM, black solid line), $\eta = 10^{-6}$ (red dash-dotted line), $\eta = 10^{-4}$ (green dashed line), and $\eta = -10^{-6}$ (blue dotted line).

side of the matter in the framework of EMSG is the principal reason for amplifying the growth of matter perturbations relative to the ΛCDM model.

In this regards, by serving the growth function as [63]

$$f(a) = \frac{dlnD}{dlna}, \qquad D(a) = \frac{\delta_m(a)}{\delta_m(a=1)}, \tag{34}$$

one can investigate the growth rate of matter perturbations. Let us recall that, in the absence of the EMSG model parameter ($\eta = 0$), the growth function is a constant of unity. In Fig. 4, we display the growth function in terms of the redshift parameter. First, like the ΛCDM model, we observe that the amplitude of perturbations in high redshifts approaches unity, while it starts to decrease at low redshifts. It means that the role of the EMSG model parameter is not in conflict with Λ to reduce the growth function from unity. Besides, the current value of $f(z)$ crucially depends on the η parameter so that, by increasing it, $f(z)$ deviates more from ΛCDM model.

There is also another possibility of measuring the growth rate matter perturbations, which come from the redshift-space distortion of the clustering pattern of galaxies. This distortion is caused by the odd velocity of the inward collapse motion of the large-scale structure, which is directly linked to the growth rate of the matter density contrast δ_m [64]. The recent surveys of galaxy redshift have provided bounds on the growth rate $f(z)$ or $f(z)\sigma_8(z)$ in terms of the redshift, where $f(z)$ comes from Eq. (34) and σ_8 is the rms (root mean square) amplitude of δ_m at the

[4]Already also discussed in Ref. [19] is the unsatisfactory behavior of $\eta < 0$ in other contexts and the possibility of its discarding in case of repeating such an unrealistic physical result.

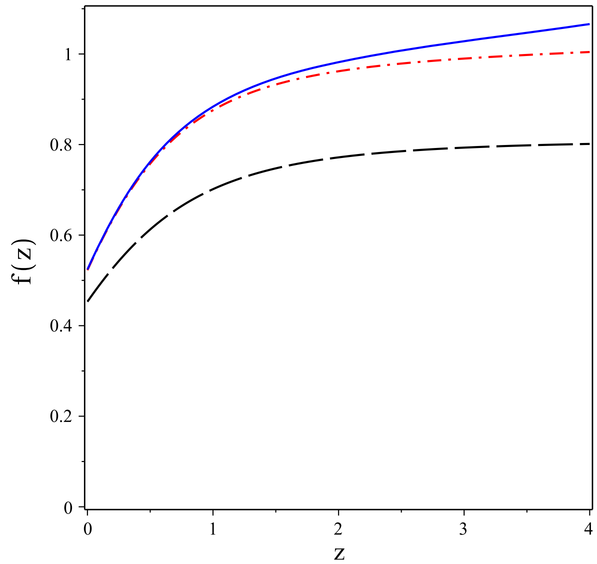

FIG. 4. The evolution of the growth function for different values of the EMSG model parameter η: $\eta = 0$ (ΛCDM, black long-dashed line), $\eta = 10^{-9}$ (red dash-dotted line), and $\eta = 10^{-8}$ (blue solid line).

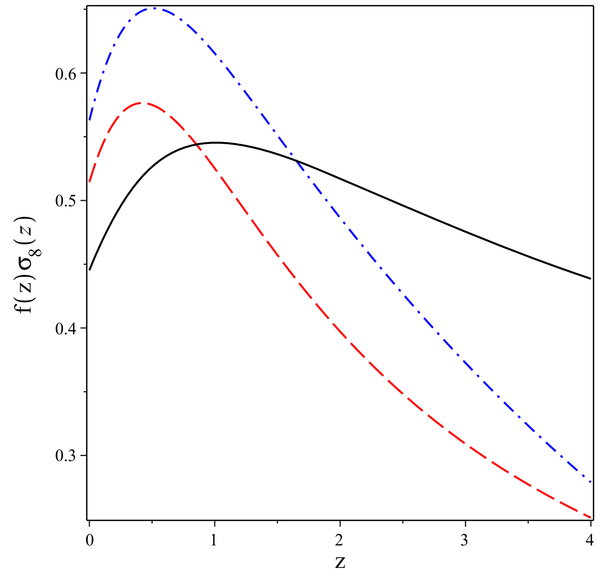

FIG. 5. The behavior of $f(z)\sigma_8(z)$ for different values of the EMSG model parameter η: $\eta = 0$ (ΛCDM, black solid line), $\eta = 10^{-8}$ (red dashed line), and $\eta = 10^{-6}$ (blue dash-dotted line).

comoving scale $8h^{-1}$ Mpc [65,66] and can be written as [67]

$$\sigma_8(z) = \frac{\delta(z)}{\delta(z=0)}\sigma_8(z=0). \qquad (35)$$

With this supposition[5] that $\sigma_8(z=0) = 0.983$ [66], we release the redshift evolution of $f(z)\sigma_8(z)$ for different values of η in Fig. 5. While in small redshifts ($z < 1$) the EMSG model with a larger η predicts a larger value of the cosmological growth rate, by going to large redshifts the behavior of models turns the same. Indeed by adding the quadratic contributions to gravity from matter terms in the EMSG model, we observe from Fig. 5 that in small redshifts the growth rate function is larger than the ΛCDM model. With the presence of EMSG model parameter η, we also see that $f\sigma_8$ reaches the maximum value at redshifts smaller than ΛCDM. Namely, the large structures form in the EMSG model later than the standard counterpart.

IV. NUMBER OF GALAXY CLUSTER IN EMSG COSMOLOGY

In addition to the evolution of matter density contrast, another quantity that we are interested in surveying in the framework of EMSG cosmology is the number count of collapsed objects. This section indeed studies the distribution of the number density of collapsed objects of a given mass range in the framework of EMSG cosmology. The collapsed objects, which, in essence, are the chief source of large-scale structure formation of the Universe, are called DM halos. Besides, the baryonic matter, due to gravitational attraction, follows the DM distribution. In this way, tracing the distribution of DM halos becomes possible by seeing the distribution of galaxy clusters. To do so, i.e., the investigation of the number distribution of the collapsed objects or the galaxy clusters along the redshift commonly a semianalytic approach known as the Press-Schechter formalism is employed [68]. From the view of the mathematical formulations of the halo mass function, the matter density field usually should enjoy the Gaussian distribution.

The comoving number density of the gravitationally collapsed objects (equivalent to galaxy clusters) at a certain redshift z having mass from M to $M + dM$ is given by the following analytical formula [69]:

$$\frac{dn(M,z)}{dM} = -\frac{\rho_{m,0}}{M}\frac{d\ln\sigma(M,z)}{dM} f(\sigma(M,z)), \qquad (36)$$

where $\rho_{m,0}$, $\sigma(M,z)$, and $f(\sigma)$, respectively, denote the present matter mean density of the Universe, the rms of density fluctuation in a sphere of radius r surrounding a mass M, and the mathematical mass function proposed by Press and Schechter [68], as follows:

$$f_{PS}(\sigma) = \sqrt{\frac{2}{\pi}}\frac{\delta_c(z)}{\sigma(M,z)}\exp\left[-\frac{\delta_c^2(z)}{2\sigma^2(M,z)}\right]. \qquad (37)$$

[5]Throughout this manuscript the values of Hubble constant H_0 and the σ_8 are fixed at the Planck-ΛCDM measurements as $H_0 = 67.66 \pm 0.42$ km s^{-1} Mpc^{-1} and $\sigma_8 = 0.983 \pm 0.0060$ (CMB power spectra + CMB lensing + BAO) [66].

Subscript "PS" refers to Press and Schechter. Note that $\delta_c(z)$ in the mass function above is the critical density contrast above which structures collapse. By serving the linearized growth factor $D(z) = \delta_m(z)/\delta_m(z=0)$, as well as the rms of density fluctuation at a fixed length $r_8 = 8h^{-1}$ Mpc, then $\sigma(M, z)$ is expressed as follows:

$$\sigma(z, M) = \sigma(0, M_8)\left(\frac{M}{M_8}\right)^{-\frac{\gamma}{3}} D(z), \tag{38}$$

where the index γ is reads as [70,71]

$$\gamma = (0.3\Omega_{m,0}h + 0.2)\left[2.92 + \frac{1}{3}\log\left(\frac{M}{M_8}\right)\right], \tag{39}$$

and $M_8 = 6\times 10^{14}\Omega_M^{(0)} h^{-1} M_\odot$ is the mass inside a sphere of radius r_8 ($M_\odot$ is the solar mass) [72].

We first in Fig. 6 display the redshift evolution of mass function $[dn/dM(1/\mathrm{Mpc}^3)]$ of objects with mass $10^{13}h^{-1}M_\odot$ for different values of EMSG model parameter η. It is important since this is one of the quantities involved in the number of DM halos. Figure 6 explicitly shows that the presence of the η causes the growth of the mass function to start around redshift less than the ΛCDM model; i.e., the halo abundance is formed later. Namely, as the parameter η becomes larger, the halo abundance grows rapidly at lower redshifts.

Finally, to survey the number of DM halos in EMSG cosmology, we employ the effective number of collapsed objects between a given range of mass bin $M_{\mathrm{inf}} < M < M_{\mathrm{sup}}$ per unit of redshift:

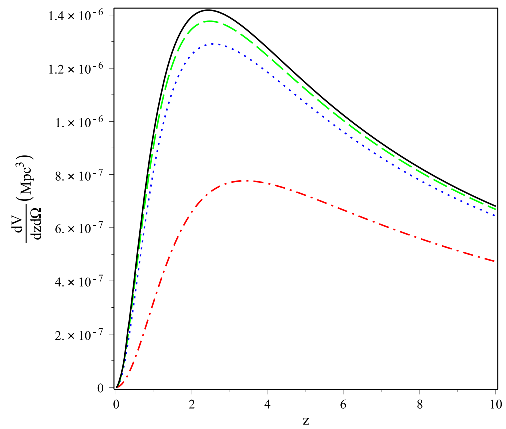

FIG. 7. The behavior of the comoving volume element with different values of the EMSG model parameter η: $\eta = 0$ (ΛCDM, black solid curve), $\eta = 10^{-5}$ (green dashed curve), $\eta = 10^{-4}$ (blue dotted curve), and $\eta = 10^{-3}$ (red dash-dotted curve).

$$\mathcal{N}^{bin} \equiv \frac{dN}{dz} = \int_{4\pi} d\Omega \int_{M_{\mathrm{inf}}}^{M_{\mathrm{sup}}} \frac{dn}{dM}\frac{dV}{dzd\Omega} dM, \tag{40}$$

where $\frac{dV}{dzd\Omega}$ is the comoving volume element and is defined as

$$\frac{dV(z)}{dzd\Omega} = \frac{r^2(z)}{H(z)}, \qquad r(z) = \int_0^z H^{-1}(x)dx. \tag{41}$$

Here $r(z)$ denotes the comoving distance. We depict the redshift evolution of the comoving volume element $[dV/dzd\Omega(\mathrm{Mpc}^3)]$ with various values of the EMSG

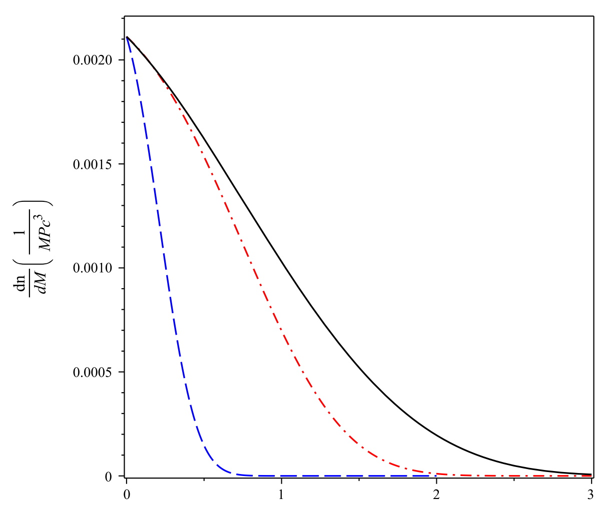

FIG. 6. The evolution of mass function for objects with mass $M = 10^{13}(h^{-1}M_\odot)$ and different values of the EMSG model parameter η: $\eta = 0$ (ΛCDM, black solid line), $\eta = 10^{-5}$ (red dash-dotted line), and $\eta = 10^{-3}$ (blue dashed line). In general, for objects with the mass range 10^{13}–$10^{16}h^{-1}M_\odot$, we are faced with this same qualitative behavior.

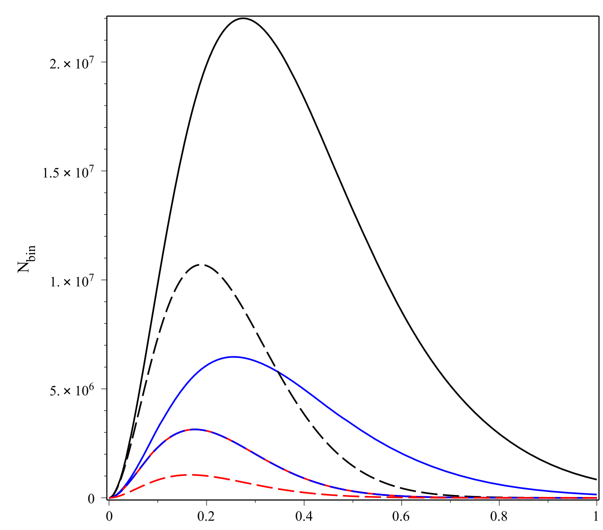

FIG. 8. The evolution of cluster number count with redshift from the ΛCDM (solid curves), and EMSG with $\eta = 10^{-5}$ (dashed curves), for objects with mass within the range: $10^{12} < M/(h^{-1}M\odot) < 10^{13}$ (black), $10^{13} < M/(h^{-1}M\odot) < 10^{14}$ (blue), and $10^{14} < M/(h^{-1}M\odot) < 10^{15}$ (red).

model parameter η in Fig. 7. As we see, the comoving volume element becomes smaller in the presence of the η parameter. It is worth noting that the comoving volume element just depends on the cosmological background and the growth factor of the perturbation $D(z)$ does not affect it. By setting a certain value for EMSG model parameter η, as well as taking ΛCDM into account, for various mass bins $[M_{\rm inf}, M_{\rm sup}]$ from $10^{12}h^{-1}M_\odot$ to $10^{15}h^{-1}M_\odot$, we display in Fig. 8 the behavior of $\mathcal{N}^{bin} - z$ (the number count in mass bins). It has two clear messages. First of all, the cluster number count in the presence of the EMSG model parameter is less than its standard counterpart. Second, the more massive structures are less abundant and form at later times which is in agreement with what we expect from the hierarchical model of structure formation.

V. CONCLUSION

It is well known that utilizing the SC formalism of matter's overdensity is a suitable method to study the effects of "modified gravity" on the large-scale structure of the Universe. In the present work, by serving SC formalism, we have studied the linear evolution of matter's overdensity in the cosmology framework arising from EMSG, which affects the behavior of standard ΛCDM in the early Universe due to inducing quadratic contributions from matter to gravity. These corrections affect the expansion history of the Universe, too. In practical phenomenological terms, one may imagine it as a potential extension of the ΛCDM model of cosmology. More precisely, using Friedmann dynamics equations (in the presence of a cosmological constant) modified with terms containing EMSG model parameter η, and by taking into account these new effects on the growth of perturbations, we have investigated the structure formation beyond ΛCDM.

It is well known from standard cosmology that the Universe in the past around a redshift z_{tr} has been switched from a decelerated phase to an accelerated phase, and it continues today. We found that the presence of η terms in dynamics of EMSG cosmology affects the value of z_{tr} so that it increases (decreases) with $\eta > 0$ ($\eta < 0$) meaning that our Universe experiences this phase transition sooner (later) than ΛCDM. Our evaluation of the evolution of the matter density contrast for different values of η ruled out case $\eta < 0$ and showed that the matter density contrast grows up faster than the ΛCDM profile. It is, in essence, due to nonlinear matter extensions appearing in the dynamics of EMSG cosmology. The growth function increases in the presence of the EMSG model parameter η, too. In this regard, we have investigated $f\sigma_8$ for EMSG cosmology and found that, in the presence of η parameter, $f\sigma_8$ reaches the maximum value at smaller redshifts. Namely, the large-scale structures in the framework of EMSG cosmology form later compared to ΛCDM.

The modifications caused by EMSG cosmology affect the number of DM halos so that the presence of η makes halo abundances smaller than ΛCDM. In other words, for larger η, the mass function starts to grow in smaller redshifts, meaning that the halo abundance is formed later relative to ΛCDM. The comoving volume element becomes smaller in EMSG cosmology, too. In addition, in light of analyzing the number counts in mass bins for the cosmology model at hand, two results were obtained. First, the number of galaxy clusters in EMSG is less than the ΛCDM model. Second, we found that in EMSG more massive structures are less abundant and form at later times, as expected from the hierarchical model of structure formation.

The present study shows that the evolution of linear perturbation reacts to the EMSG model parameter and it leaves distinguishable imprints from ΛCDM. For this reason, the outputs of such studies would be helpful to constrain the models based on future observations like type Ia supernovas and baryon acoustic oscillations, etc.

[1] D. H. Weinberg, M. J. Mortonson, D. J. Eisenstein, C. Hirata, A. G. Riess, and E. Rozo, Phys. Rep. **530**, 87 (2013).

[2] S. Capozziello and M. De Laurentis, Phys. Rep. **509**, 167 (2011).

[3] S. Nojiri, S. D. Odintsov, and V. K. Oikonomou, Phys. Rep. **692**, 1 (2017).

[4] G. Cognola, E. Elizalde, S. Nojiri, S. D. Odintsov, L. Sebastiani, and S. Zerbini, Phys. Rev. D **77**, 046009 (2008).

[5] T. Harko, F. Lobo, S. Nojiri, and S. Odintsov, Phys. Rev. D **84**, 024020 (2011).

[6] Z. Haghani, T. Harko, F. S. N. Lobo, H. R. Sepangi, and S. Shahidi, Phys. Rev. D **88**, 044023 (2013).

[7] R. Myrzakulov, arXiv:1205.5266.

[8] T. Harko and F. Lobo, Galaxies **2**, 410 (2014).

[9] R. Zaregonbadi, M. Farhoudi, and N. Riazi, Phys. Rev. D **94**, 084052 (2016).

[10] H. Velten and T. R. P. Caramês, Phys. Rev. D **95**, 123536 (2017).

[11] N. Katirci and Mehmet Kavuk, Eur. Phys. J. Plus **129**, 163 (2014).

[12] K. Freese and M. Lewis, Phys. Lett. B **540**, 1 (2002).

[13] Ö. Akarsu, N. Katırci, and S. Kumar, Phys. Rev. D **97**, 024011 (2018).

[14] M. Roshan and F. Shojai, Phys. Rev. D **94**, 044002 (2016).

[15] C. Board and J. Barrow, Phys. Rev. D **96**, 123517 (2017).
[16] O. Akarsu, N. Katirci, S. Kumar, R. C. Nunes, and M. Sami, Phys. Rev. D **98**, 063522 (2018).
[17] O. Akarsu and N. M. Uzun, Phys. Dark Universe **40**, 101194 (2023).
[18] O. Akarsu, E. Nazari, and M. Roshan, arXiv:2302.04682.
[19] O. Akarsu, J. D. Barrow, S. Çıkıntoğlu, K. Yavuz Ekşi, and N. Katirci, Phys. Rev. D **97**, 124017 (2018).
[20] M. Khodadi, A. Allahyari, and S. Capozziello, Phys. Dark Universe **36**, 101013 (2022).
[21] M. Sharif and M. Zeeshan Gul, Phys. Scr. **96**, 105001 (2021).
[22] M. Sharif and M. Zeeshan Gul, Universe **9**, 145 (2023).
[23] A. H. Barbar, A. M. Awad, and M. T. AlFiky, Phys. Rev. D **101**, 044058 (2020).
[24] E. Nazari, F. Sarvi, and M. Roshan, Phys. Rev. D **102**, 064016 (2020).
[25] S. Weinberg, Rev. Mod. Phys. **61**, 1 (1989).
[26] T. Padmanabhan, Phys. Rep. **380**, 235 (2003).
[27] G. B. Zhao, M. Raveri, L. Pogosian, Y. Wang, R. G. Crittenden, W. J. Handley, W. J. Percival, F. Beutler, J. Brinkmann, C. H. Chuang *et al.*, Nat. Astron. **1**, 627 (2017).
[28] J. S. Bullock and M. Boylan-Kolchin, Annu. Rev. Astron. Astrophys. **55**, 343 (2017).
[29] E. Di Valentino, Nat. Astron. **1**, 569 (2017).
[30] E. Abdalla, G. Franco Abellán, A. Aboubrahim, A. Agnello, O. Akarsu, Y. Akrami, G. Alestas, D. Aloni, L. Amendola, L. A. Anchordoqui *et al.*, J. High Energy Astrophys. **34**, 49 (2022).
[31] M. Khodadi and M. Schreck, Phys. Dark Universe **39**, 101170 (2023).
[32] J. P. Hu and F. Y. Wang, Universe **9**, 94 (2023).
[33] B. H. Lee, W. Lee, E. Ó. Colgáin, M. M. Sheikh-Jabbari, and S. Thakur, J. Cosmol. Astropart. Phys. 04 (2022) 004.
[34] A. Banerjee, H. Cai, L. Heisenberg, E. Ó. Colgáin, M. M. Sheikh-Jabbari, and T. Yang, Phys. Rev. D **103**, L081305 (2021).
[35] H. R. Fazlollahi, Eur. Phys. J. Plus **138**, 211 (2023).
[36] C. Ranjit, P. Rudra, and S. Kundu, Ann. Phys. (Amsterdam) **428**, 168432 (2021).
[37] M. Faraji, N. Rashidi, and K. Nozari, Eur. Phys. J. P **137**, 5 (2022).
[38] E. Nazari, M. Roshan, and I. De Martino, Phys. Rev. D **105**, 044014 (2022).
[39] E. Nazari, Phys. Rev. D **105**, 104026 (2022).
[40] P. H. R. S. Moraes and P. K. Sahoo, Phys. Rev. D **97**, 024007 (2018).
[41] M. C. F. Faria, C. J. A. P. Martins, F. Chiti, and B. S. A. Silva, Astron. Astrophys. **625**, A127 (2019).
[42] S. Bahamonde, M. Marciu, and P. Rudra, Phys. Rev. D **100**, 083511 (2019).
[43] S. Shahidi, Eur. Phys. J. C **81**, 274 (2021).
[44] E. Kolonia and C. Martins, Phys. Dark Universe **36**, 101021 (2022).
[45] M. Khodadi and J. T. Firouzjaee, Phys. Dark Universe **37**, 101084 (2022).
[46] M. Sharif and M. Z. Gul, Mod. Phys. Lett. A **37**, 2250005 (2022).
[47] M. Sharif and M. Zeeshan Gul, J. Exp. Theor. Phys. **136**, 436 (2023).
[48] M. Sharif and S. Naz, Ann. Phys. (Amsterdam) **451**, 169240 (2023).
[49] R. Abramo, R. Batista, L. Liberato, and R. Rosenfeld, J. Cosmol. Astropart. Phys. 11 (**2007**) 012.
[50] J. E. Gunn and J. R. Gott, III, Astrophys. J. **176**, 1 (1972).
[51] S. Planelles, D. Schleicher, and A. Bykov, Space Sci. Rev. **51**, 93 (2016).
[52] A. Ziaie, H. Shabani, and S. Ghaffari, Mod. Phys. Lett. A **36**, 2150082 (2021).
[53] A. H. Ziaie, H. Moradpour, and H. Shabani, Eur. Phys. J. Plus **135**, 916 (2020).
[54] B. Farsi and A. Sheykhi, Phys. Rev. D **106**, 024053 (2022).
[55] A. Sheykhi and B. Farsi, Eur. Phys. J. C **82**, 1111 (2022).
[56] B. Farsi and A. Sheykhi, arXiv:2301.13263.
[57] R. L. Munoz and M. Bruni, Phys. Rev. D **107**, 123536 (2023).
[58] F. G. Alvarenga, A. de la Cruz-Dombriz, M. J. S. Houndjo, M. E. Rodrigues, and D. Sáez-Gómez, Phys. Rev. D **87**, 103526 (2013).
[59] M. Sharif and M. Zeeshan Gul, Int. J. Mod. Phys. A **36**, 2150004 (2021).
[60] A. Ashtekar and P. Singh, Classical Quantum Gravity **28**, 213001 (2011).
[61] P. Brax and C. van de Bruck, Classical Quantum Gravity **20**, R201 (2003).
[62] B. Ryden, *Introduction to Cosmology* (Addison-Wesley Press, San Francisco, 2003).
[63] P. Peebles, *Principles of Physical Cosmology* (Princeton University Press, Princeton, NJ, 1993).
[64] N. Kaiser, Mon. Not. R. Astron. Soc. **227**, 1 (1987).
[65] S. Tsujikawa, A. Felice, and J. Alcaniz, J. Cosmol. Astropart. Phys. 01 (2013) 030.
[66] S. Nesseris, G. Pantazis, and L. Perivolaropoulos, Phys. Rev. D **96**, 023542 (2017).
[67] S. Nesseris and L. Perivolaropoulos, Phys. Rev. D **77**, 023504 (2008).
[68] H. William and P. Schechter, Astrophys. J. **187**, 425 (1974).
[69] L. Liberato and R. Rosenfeld, J. Cosmol. Astropart. Phys. 07 (2006) 009.
[70] A. Mukherjee, arXiv:2008.03792.
[71] A. Mukherjee, arXiv:2008.08979.
[72] P. T. P. Viana and A. R. Liddle, Mon. Not. R. Astron. Soc. **281**, 323 (1996).